

# Wld<sup>S</sup> Prevents Axon Degeneration through Increased Mitochondrial Flux and Enhanced Mitochondrial Ca<sup>2+</sup> Buffering

Michelle A. Avery,<sup>1</sup> Timothy M. Rooney,<sup>1</sup> Jignesh D. Pandya,<sup>3</sup> Thomas M. Wishart,<sup>2</sup> Thomas H. Gillingwater,<sup>2</sup> James W. Geddes,<sup>3</sup> Patrick G. Sullivan,<sup>3</sup> and Marc R. Freeman<sup>1,\*</sup>

<sup>1</sup>Department of Neurobiology, University of Massachusetts Medical School, and Howard Hughes Medical Institute, Worcester, MA 01605-2324, USA

<sup>2</sup>Euan MacDonald Centre for Motor Neurone Disease Research and Centre for Integrative Physiology, University of Edinburgh, Edinburgh, EH8 9XD, UK

<sup>3</sup>Spinal Cord and Brain Injury Research Center, Department of Anatomy and Neurobiology, University of Kentucky, Lexington, KY 40536-0509, USA

## Summary

Wld<sup>S</sup> (slow Wallerian degeneration) is a remarkable protein that can suppress Wallerian degeneration of axons and synapses [1], but how it exerts this effect remains unclear [2]. Here, using *Drosophila* and mouse models, we identify mitochondria as a key site of action for Wld<sup>S</sup> neuroprotective function. Targeting the NAD<sup>+</sup> biosynthetic enzyme Nmnat to mitochondria was sufficient to fully phenocopy Wld<sup>S</sup>, and Wld<sup>S</sup> was specifically localized to mitochondria in synaptic preparations from mouse brain. Axotomy of live wild-type axons induced a dramatic spike in axoplasmic Ca<sup>2+</sup> and termination of mitochondrial movement—Wld<sup>S</sup> potently suppressed both of these events. Surprisingly, Wld<sup>S</sup> also promoted increased basal mitochondrial motility in axons before injury, and genetically suppressing mitochondrial motility in vivo dramatically reduced the protective effect of Wld<sup>S</sup>. Intriguingly, purified mitochondria from Wld<sup>S</sup> mice exhibited enhanced Ca<sup>2+</sup> buffering capacity. We propose that the enhanced Ca<sup>2+</sup> buffering capacity of Wld<sup>S</sup> mitochondria leads to increased mitochondrial motility, suppression of axotomy-induced Ca<sup>2+</sup> elevation in axons, and thereby suppression of Wallerian degeneration.

## Results and Discussion

### Mitochondria as a Key Site of Wld<sup>S</sup> Neuroprotective Function

Remarkably, the distal fragments of severed axons survive for weeks after axotomy in the Wld<sup>S</sup> (slow Wallerian degeneration) mouse [3–6]. The Wld<sup>S</sup> mutation resulted from the fusion of two neighboring genes and led to the production of a novel hybrid protein (Wld<sup>S</sup>) composed of the 70 NH-terminal amino acids of the E4 ubiquitin ligase Ube4b, a novel 18 amino acid linker domain, and the NAD<sup>+</sup> biosynthetic enzyme Nmnat1 [7]. We previously found that expression of mouse Nmnat3 in *Drosophila* olfactory receptor neuron (ORN) axons provided protection equivalent to Wld<sup>S</sup> 5 days after axotomy [8]. Recent work has shown that Nmnat3 expression in mouse neurons also robustly protects axons [9]. We coexpressed mouse

UAS-Nmnat3::Myc and the mitochondrial marker UAS-mito::GFP in *Drosophila* ORNs. We found Nmnat3::Myc localized in a punctate pattern in ORN axons that precisely overlapped with mito::GFP (Figure 1A), indicating that Nmnat3 localized predominantly, if not exclusively, to mitochondria. We next assayed ORN axon preservation at 10, 20, and 50 days after axotomy. We found that Nmnat3 protected axons at levels indistinguishable from Wld<sup>S</sup> at all time points tested (Figure 1B). Thus the N70 and W18 domains of Wld<sup>S</sup> are dispensable for axon protection if Nmnat activity is targeted to mitochondria. By contrast, expression of Nmnat2 in ORN axons failed to suppress Wallerian degeneration, despite the fact that Nmnat2::Myc was localized throughout the axonal compartment (see Figure S1A available online).

Recently Yahata et al. [9] reported that in mouse neurons, Wld<sup>S</sup> protein is located in mitochondria, cytosol, peroxisome/lysosome, and endoplasmic reticulum (ER) and/or Golgi-enriched cell fractions. We revisited Wld<sup>S</sup> localization in isolated mouse striatum from control and Wld<sup>S</sup> mice by separating the tissues into three fractions: nonsynaptic striatal tissue, striatal synaptosomes without mitochondria, and synaptic mitochondria. We found that Wld<sup>S</sup> was detectable in the nonsynaptic fraction, as would be expected from its predominantly nuclear localization. In addition, we detected Wld<sup>S</sup> in synaptic mitochondria, but not in mitochondria-free synaptic preparations (Figure S1B). These data are consistent with a primarily mitochondrial localization of Wld<sup>S</sup> in axons and synapses in vivo in mouse brain.

### Wld<sup>S</sup> Suppresses Termination of Mitochondrial Motility after Injury and Axotomy-Induced Increases in Axonal Ca<sup>2+</sup>

We assayed mitochondrial dynamics in live *Drosophila* axons using the *Tdc2-Gal4* driver, which is expressed in only three axons per segment of larval peripheral nerve, by driving UAS-*mCD8::mCherry* (to label axonal membranes) and UAS-*mito::GFP* (to label mitochondria; Figure 3A). In uninjured axons, we found no differences in the total number of mitochondria, mitochondrial morphology, or mitochondrial size when we compared control and Wld<sup>S</sup>-expressing axons (Figures S1A and S1B). In control animals we found that ~35% of mitochondria were motile before injury, but all motility terminated after laser axotomy (Movie S1). In striking contrast, we found that laser axotomy of Wld<sup>S</sup>-expressing axons had no effect on mitochondrial movement (Movie S2; Figure 1C).

Axon injury in mammals leads to extracellular Ca<sup>2+</sup> entry, which is necessary and sufficient for Wallerian degeneration [10]. Mitochondrial motility is known to be potently modulated by Ca<sup>2+</sup> [11, 12]. We therefore sought to determine whether *Drosophila* axons showed axotomy-induced changes in axonal Ca<sup>2+</sup>, and whether axonal Ca<sup>2+</sup> signaling was modulated by Wld<sup>S</sup>. We drove the expression of the genetically encoded Ca<sup>2+</sup> indicator GCaMP3 in axons and measured changes in GCaMP3 signals in distal axon segments after laser-induced axotomy. In control animals, we found a rapid increase in Ca<sup>2+</sup> levels within seconds after axotomy, with Ca<sup>2+</sup> levels peaking within 1 min after cut, and then returning toward baseline levels over the next hour (Figures 2A–2C;

\*Correspondence: marc.freeman@umassmed.edu

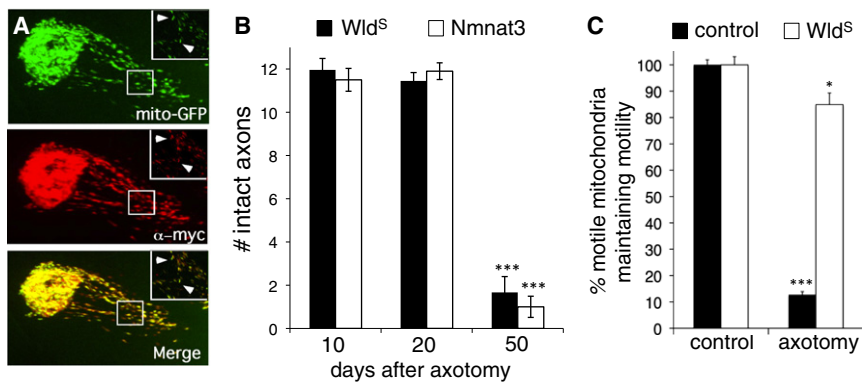


Figure 1. Mitochondria as a Focal Point for  $Wid^S$ -Mediated Axon Protection

(A) Mouse  $Nmnat3::Myc$  localizes to mitochondria in *Drosophila* axons. *22a-Gal4* was used to drive *UAS-Nmnat3::Myc* and *UAS-mito::GFP*. Insets show boxed region.

(B) Mitochondrial  $Nmnat3$  fully mimics  $Wid^S$  in axon protective function. *22a-Gal4* was used to drive *UAS-Nmnat3* or *UAS-Wid<sup>S</sup>* in a background where axons were labeled with membrane-tethered GFP (*UAS-mCD8::GFP*).  $n \geq 20$  antennal lobes for each. \*\*\* $p < 0.001$ . Error bars represent  $\pm$  SEM.

(C)  $Wid^S$  suppresses axotomy-induced termination of mitochondrial motility. Mitochondrial movement was assessed in live open-filet preparations of third-instar *Drosophila* larvae

immediately after axotomy for 5 min. Axotomy was induced by severing axons with a Micropoint laser ablation system and confirmed by a breakage of  $mCD8::mCherry$ -labeled axons.  $n \geq 10$  live samples for each genotype and time point. \*\*\* $p < 0.001$ .

Movie S3). However, >1 hr after axotomy, axonal  $Ca^{2+}$  levels remained significantly elevated above baseline (~20% increase). Strikingly, whereas baseline  $Ca^{2+}$  levels in  $Wid^{S+}$  axons were indistinguishable from those in controls (Figure S3C), in  $Wid^{S+}$  axons, injury-induced  $Ca^{2+}$  bursts were almost completely eliminated:  $Ca^{2+}$  levels only rose to ~15% control levels and returned to baseline within 1.5 min (Figure 2C; Movie S4).

In previous work, we generated a collection of *UAS*-regulated  $Wid^S$ -derived molecules that suppress Wallerian degeneration to varying degrees [8] (Figure S1C). We assayed axotomy-induced changes in GCaMP3 fluorescence in axons expressing each of these molecules in live larval preparations. As with  $Wid^S$ , we found no evidence for changes in axonal mitochondrial number, morphology, or size in these backgrounds (Figures S2A and S2B). However, we found a striking correlation between axon protective function and suppression of axotomy-induced increases in axonal  $Ca^{2+}$ :  $Wid^S$  and  $Nmnat3$  strongly suppressed Wallerian degeneration and postinjury axonal  $Ca^{2+}$  increases;  $Nmnat1$ ,  $\Delta N16::Wid^S$ ,

and  $Wid^{S-dead}$  partially suppressed Wallerian degeneration and postinjury axonal  $Ca^{2+}$  increases;  $Nmnat1^{dead}$ , which lacks  $NAD^+$  biosynthetic activity and provided no protection from Wallerian degeneration [8], did not affect postinjury axonal  $Ca^{2+}$  increases. These changes were evident in both the distal and proximal axon segment and affected both peak axonal  $Ca^{2+}$  intensities and recovery times to baseline  $Ca^{2+}$  levels (Figures 2C–2E; Figures S3A and S3B).

### $Wid^S$ Enhances Mitochondrial Movement, which Is Essential for Maximal Axonal Protection after Injury

Because mitochondrial motility is  $Ca^{2+}$ -modulated, we reasoned that changes in axonal  $Ca^{2+}$  buffering might affect axonal mitochondrial motility. We therefore assayed mitochondrial flux in axons expressing  $Wid^S$ -derived neuroprotective molecules. Surprisingly, we found a significant change in basal mitochondrial motility: in control animals, ~35% of total axonal mitochondria were motile; however, ~65% of mitochondria were motile in  $Wid^{S+}$  axons. Moreover, we found that molecules that provide partial suppression of Wallerian

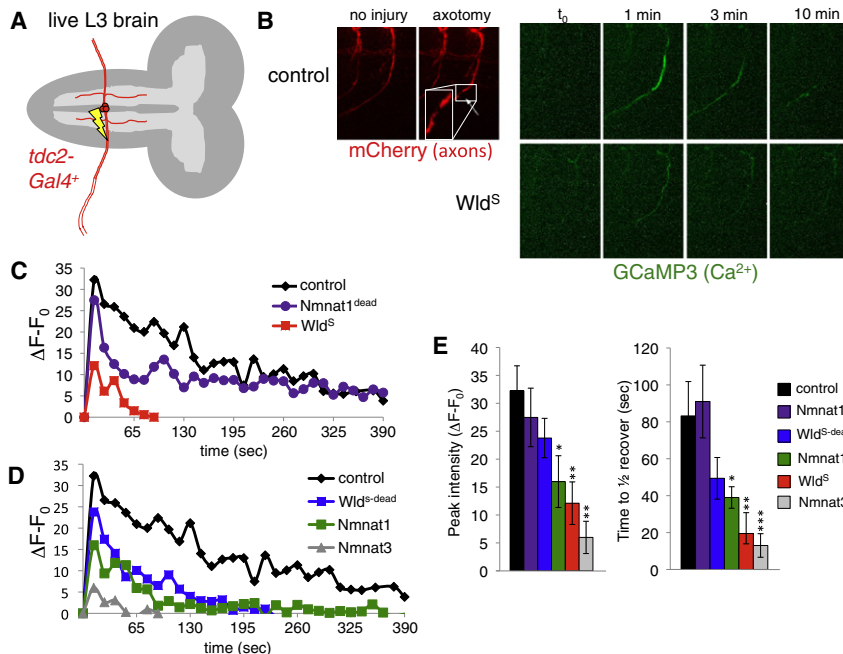


Figure 2. In Vivo Laser Axotomy Induces a Dramatic Rise in Axonal  $Ca^{2+}$  that Is Suppressed by  $Wid^S$

(A) *tdc2-Gal4* labels three axons in each peripheral nerve; only one segment is illustrated.

(B) Axons were labeled with  $mCD8::mCherry$ , and axonal  $Ca^{2+}$  was monitored by coexpressing GCaMP3 in the *tdc2-Gal4+* subset of neurons. Note the breakage of the axon after laser axotomy (red,  $mCherry$ ). Axonal  $Ca^{2+}$  levels 1 min after axotomy (green, GCaMP3).

(C and D) Representative traces showing  $Ca^{2+}$  responses in axon fragments distal to the injury site over time. Genotypes as indicated.

(E) Quantification of peak  $Ca^{2+}$  intensities and time to one-half recovery from average peak intensity for each genotype listed.  $n \geq 5$  live samples for each genotype and time point versus control. \* $p < 0.05$ ; \*\* $p < 0.01$ ; \*\*\* $p < 0.001$ .

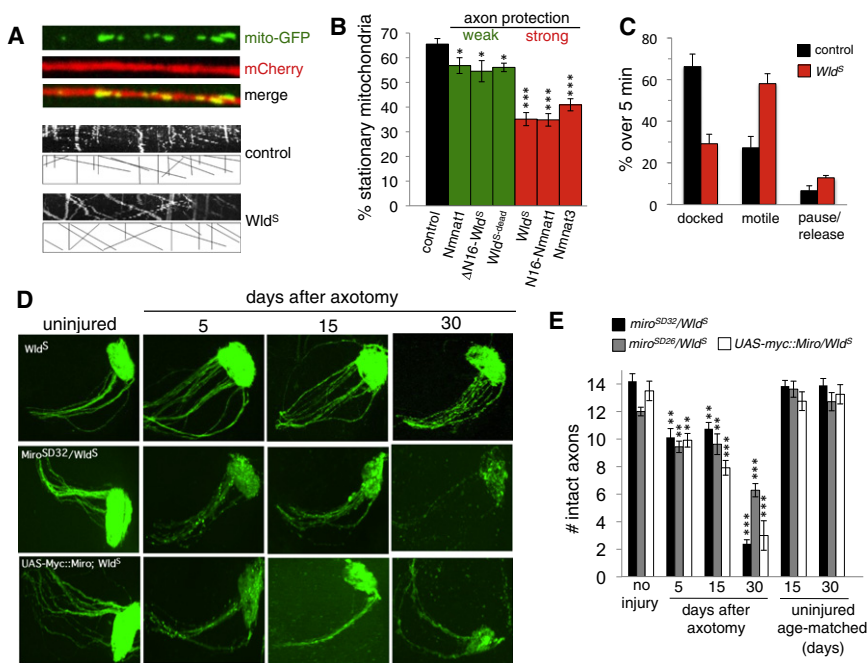


**Figure 3. Wld<sup>S</sup> Increases Mitochondrial Flux, which Is Essential for Neuroprotective Function**  
(A) Mitochondrial flux was assayed in *tdc2-Gal4*-expressing neurons in live preparations of third-instar larvae. Representative kymographs of mitochondrial movement are shown for control and Wld<sup>S</sup>-expressing axons. Anterograde is to the right, retrograde is to the left.  
(B) Mitochondrial flux was assayed in axons expressing each of the following molecules: Nmnat1, DN16-Wld<sup>S</sup>, Wld<sup>S-dead</sup>, Wld<sup>S</sup>, N16-Nmnat1, and Nmnat3. n ≥ 10 live samples for each genotype. \*p < 0.05; \*\*\*p < 0.001.  
(C) Quantification of the movement of individual mitochondria by binning into mobile, docked, or pausing and/or releasing during a 5 min window. n = 5 movies for each genotype.  
(D) ORN axotomy assays in Wld<sup>S</sup> backgrounds and *miro* mutants. A single antennal lobe where ORN axons were severed is shown.  
(E) Quantification of data from (D). Age-matched uninjured controls at the same time points are shown at right. n ≥ 15 samples for each genotype and time point. \*\*p < 0.01; \*\*\*p < 0.001.

degeneration (Nmnat1,  $\Delta$ N16::Wld<sup>S</sup>, and Wld<sup>S-dead</sup>) led to a modest, but significant, increase in the number of motile mitochondria, whereas molecules that maximally suppress Wallerian degeneration (Wld<sup>S</sup>, N16::Nmnat1, and Nmnat3) led to a robust increase in the number of motile mitochondria (Figure 3B). This change in mitochondrial flux in Wld<sup>S</sup> axons appears to represent a decrease in docked mitochondria, an increase in motile mitochondria, but no significant change in pause and/or release rates for individual mitochondria (Figure 3C).

Is increased mitochondrial flux critical for Wld<sup>S</sup>-mediated axon protection? The adaptor protein Miro functions to tether mitochondria to cytoskeletal motor proteins and modulate mitochondrial movement in a Ca<sup>2+</sup>-dependent fashion [12]. Impressively, mutations in *miro* dominantly decrease mitochondrial motility [13]. We therefore crossed strong alleles of *miro* (*miro*<sup>SD32</sup> and *miro*<sup>SD26</sup>) and a UAS-regulated version of Miro (*UAS-myc::Miro*), which when overexpressed acts as a dominant-negative [13], into the Wld<sup>S</sup> background and assayed mitochondrial flux. We found that *miro* mutants or expression of Myc::Miro dominantly suppressed mitochondrial movement in controls. In addition, we found that loss of Miro function also decreased mitochondrial movement in the presence of Wld<sup>S</sup> to levels found in control animals (Figures S2C and S2D). Remarkably, reduced *miro* function also dominantly suppressed the neuroprotective effects of Wld<sup>S</sup> in ORN axotomy assays. In animals with reduced *miro* function, axon loss was evident by 5 days after axotomy, with synaptic regions showing significant degeneration, and by 30 days after axotomy, the protection afforded by Wld<sup>S</sup> is almost completely blocked (Figures 3D and 3E).

**Mitochondria from Wld<sup>S</sup>-Expressing Axons Show Enhanced Ca<sup>2+</sup> Buffering Capacity and Resistance to Formation of the Permeability Transition Pore**  
Mitochondria are major sinks for cellular Ca<sup>2+</sup> in both axons and synapses [14]. A powerful mechanism by which Wld<sup>S</sup>

could exert all of these effects would be by altering mitochondrial Ca<sup>2+</sup> buffering capacity. We therefore assessed mitochondrial Ca<sup>2+</sup> cycling and/or buffering capacity in cortical mitochondria isolated from young (~p25) wild-type (WT) (NJ) and Wld<sup>S</sup> mice. Mitochondrial isolations [15, 16] from both control and Wld<sup>S</sup> animals yielded healthy, well-coupled mitochondria (Figures 4A and 4B). No apparent difference was observed in the Ca<sup>2+</sup> uptake rates in mitochondria isolated from Wld<sup>S</sup> versus control mice (Figures 4A and 4B). In contrast, the threshold for mitochondrial permeability, indicated by the loss of membrane potential (Figure 4A) and mitochondrial release of Ca<sup>2+</sup> (Figure 4B), was significantly greater in mitochondria from Wld<sup>S</sup> mice (Figure 4C). Thus, following increases in cytoplasmic Ca<sup>2+</sup>, Wld<sup>S</sup> mitochondria isolated from mouse brain buffer higher loads of Ca<sup>2+</sup> before releasing it back into the cytoplasmic compartment via the mitochondria permeability transition pore (PTP).

## Conclusions

The mechanistic action of Wld<sup>S</sup> has remained controversial, but recent work has established a nonnuclear role for Wld<sup>S</sup> [2] after injury [17]. In this study, we show that Wld<sup>S</sup> is localized to mitochondria in vivo. It is important to note that protein localization studies with Wld<sup>S</sup> must be interpreted cautiously—the primarily nuclear localization of Wld<sup>S</sup> suggested a nuclear role for Wld<sup>S</sup> and initially misled the field [2]. However, we also find that Wld<sup>S</sup> increases mitochondrial Ca<sup>2+</sup> buffering capacity and results in maintained mitochondrial motility after axotomy. Taken together, these data argue strongly that the mitochondrial compartment is a key site of action for Wld<sup>S</sup> in vivo.

We have shown that axonal injury in live *Drosophila* preparations leads to a dramatic and transient rise in axonal Ca<sup>2+</sup>. Increased axonal Ca<sup>2+</sup> has been observed in mammals after acute nerve crush [18] and entry of extracellular Ca<sup>2+</sup> is necessary and sufficient for Wallerian degeneration [10]. Impressively, Wld<sup>S</sup> expression resulted in a striking suppression of

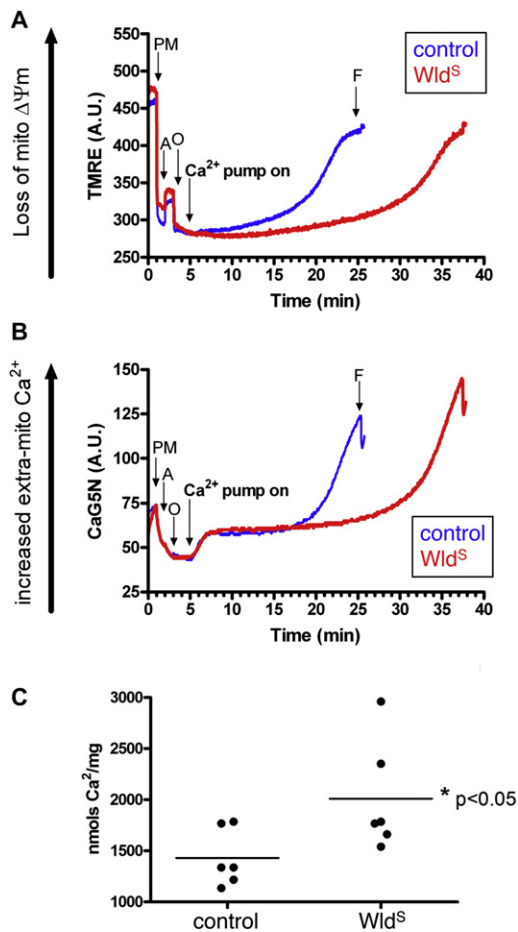


Figure 4.  $Wld^S$  Brain Mitochondria Display Higher  $Ca^{2+}$  Load Capacity than Age-Matched Wild-Type (NJ) Controls

(A and B) TMRE (tetramethylrhodamine, ethyl ester; membrane potential indicator) and CaG5N (extramitochondrial  $Ca^{2+}$  indicator) fluorescence were monitored over time simultaneously for each sample of nonsynaptic mitochondria. As illustrated in TMRE traces for the first 3 min, the addition of pyruvate and malate (PM) an oxidative substrate, causes a marked downward deflection at 1 min due to increased mitochondrial membrane potential ( $\Delta\psi_m$ ). Following ADP (A) addition, the loss of  $\Delta\psi_m$  is indicated by upward deflection at 2 min as  $\Delta\psi_m$  is utilized to phosphorylate ADP to ATP via proton flow thru the ATP synthase. The ATP synthase inhibitor, oligomycin (O) addition at 3 min results in maximum  $\Delta\psi_m$  as proton flow is inhibited. The  $Ca^{2+}$  infusion began at 5 min (infusion rate 160 nmol of  $Ca^{2+}$ /mg protein/min) and was monitored by CaG5N fluorescence and is illustrated by the initial upward deflection followed by constant signal due to mitochondrial  $Ca^{2+}$  uptake into the matrix. The subsequent rise in CaG5N fluorescence accompanied by a loss of membrane potential signifies mitochondrial permeability transition and subsequent release of mitochondrial  $Ca^{2+}$ .

(C) Quantification of mitochondrial  $Ca^{2+}$  buffering capacity (nmols/mg protein) indicates that  $Wld^S$  nonsynaptic mitochondria sequestered significantly higher amounts of  $Ca^{2+}$  compared to the control group ( $n = 6/\text{group}$ , \*  $p < 0.05$ , unpaired t test).

this axotomy-induced rise in axonal  $Ca^{2+}$ . The most plausible explanation for this enhanced buffering is that increased ATP and energy production observed in  $Wld^S$  mitochondria [9]—presumably via increased mitochondrial  $NAD^+$  production, though we cannot formally exclude essential roles for other substrates of Nmnat—is linked to increased mitochondrial membrane potential ( $\Delta\psi_m$ ), and thereby increased  $Ca^{2+}$  entry through the  $\Delta\psi_m$ -regulated mitochondrial  $Ca^{2+}$  uniporter

[19]. This model is supported by our observation that  $Wld^S$ -expressing mitochondria isolated from mouse brain exhibit an enhanced ability to maintain their membrane potential and avoid PTP formation in the face of increasing extramitochondrial  $Ca^{2+}$ . In the future, it will be important to confirm that such changes are also observed in *Drosophila* axonal mitochondrial physiology in vivo in  $Wld^S$ -expressing neurons.

Axonal  $Ca^{2+}$  spikes could result solely from entry of extracellular  $Ca^{2+}$  into the axon after injury. This would be consistent with the observation that blocking  $Ca^{2+}$  channels inhibits Wallerian degeneration [10, 18]. Mitochondria are a well-established sink for  $Ca^{2+}$  in axons [14] and here we show that  $Wld^S$  mitochondria exhibit enhanced  $Ca^{2+}$  buffering capacity and resistance to  $Ca^{2+}$ -induced formation of the permeability transition pore (PTP). Indeed PTP formation appears to be a key final execution step in Wallerian degeneration [20–22]. We therefore favor a model whereby extracellular  $Ca^{2+}$  enters the axon after axotomy and normally acts as a switch to activate Wallerian degeneration. In  $Wld^S$  axons, this  $Ca^{2+}$  is instead rapidly buffered by mitochondria, thereby blocking induction of axonal destruction. Consistent with this model, uncoupling mitochondria, which suppresses mitochondrial  $Ca^{2+}$  uptake [23, 24], completely abrogates the protective effect of  $Wld^S$  in vitro [25].

$Wld^S$ -expressing neurons exhibit a roughly 2-fold increase in the number of motile versus stationary mitochondria compared to WT controls, which could result from changes in mitochondrial  $Ca^{2+}$  buffering. Notably, genetic suppression of enhanced mitochondrial flux using mutations in *miro* also resulted in a remarkable suppression of  $Wld^S$ -mediated axonal protection in vivo. However, because this suppression was only partial, additional factors beyond increases in mitochondrial motility must also contribute to  $Wld^S$ -mediated axonal protection. For example, axonal energy supplies are likely closely intertwined with mitochondrial transport and bioenergetics.  $Wld^S$  mitochondria are known to exhibit an enhanced ability to generate ATP [9]. This change in bioenergetics, coupled with increased mitochondrial motility in  $Wld^S$  axons, might enhance distribution of ATP or other mitochondrially-derived metabolites. At the same time, enhanced mitochondrial motility could also speed the removal of metabolic byproducts normally processed by mitochondria. Similarly, increased mitochondrial motility in axons could further enhance mitochondrial  $Ca^{2+}$  buffering in  $Wld^S$  axons because motile mitochondria would be predicted to traverse more “axonal space” and perhaps be exposed to more  $Ca^{2+}$  than stationary mitochondria. Together, these could have the combined effect of increasing energy delivery, removing harmful byproducts, and increased buffering of  $Ca^{2+}$ , a signal that can potentially activate axonal degeneration.

A role for mitochondria in the  $Wld^S$  neuroprotective mechanism is intriguing because defects in mitochondria respiration and dynamics are emerging as critical underlying factors in a number of neurological disorders [26]. For example, in mouse models of ALS (SOD1 transgenics), anterograde [27] and retrograde [28] mitochondrial transport is reduced, altered mitochondrial trafficking has been observed in models of Alzheimer’s disease [29], and mutant, but not WT Huntington, protein blocks mitochondrial movement in cortical neurons [30]. However, in the majority of models, whether these mitochondrial alterations are a cause or consequence of disease remains an open question [26]. Our study shows, reciprocally, that enhanced mitochondrial flux is associated with and is required for maximal axon protection by  $Wld^S$ .

## Supplemental Information

Supplemental Information includes four figures, Supplemental Experimental Procedures, and four movies and can be found with this article online at doi:10.1016/j.cub.2012.02.043.

## Acknowledgments

All animal procedures were carried out in accordance with National Institutes of Health (NIH) guidelines and the Institutional Animal Care and Use Committee regulations of the University of Kentucky and the University of Edinburgh. This work was supported by NIH grant NS062993 (J.W.G. and P.G.S.), the Wellcome Trust (T.H.G. and M.R.F.), and NIH grant NS059991 (to M.R.F.). M.R.F. is an Early Career Scientist with the Howard Hughes Medical Institute. T.M.R. was supported by a grant from the Department of Defense (BC093796). We thank Vimala Bondada and Dingyuan Lou for preliminary work on the mitochondrial Ca<sup>2+</sup> dynamics and all members of the laboratories for helpful discussions.

Received: November 3, 2011

Revised: December 29, 2011

Accepted: February 22, 2012

Published online: March 15, 2012

## References

- Conforti, L., Tartton, A., Mack, T.G., Mi, W., Buckmaster, E.A., Wagner, D., Perry, V.H., and Coleman, M.P. (2000). A Ufd2/D4Cole1e chimeric protein and overexpression of Rbp7 in the slow Wallerian degeneration (WldS) mouse. *Proc. Natl. Acad. Sci. USA* 97, 11377–11382.
- Coleman, M.P., and Freeman, M.R. (2010). Wallerian degeneration, wld(s), and nmnat. *Annu. Rev. Neurosci.* 33, 245–267.
- Lunn, E.R., Perry, V.H., Brown, M.C., Rosen, H., and Gordon, S. (1989). Absence of Wallerian Degeneration does not Hinder Regeneration in Peripheral Nerve. *Eur. J. Neurosci.* 1, 27–33.
- Perry, V.H., Brown, M.C., Lunn, E.R., Tree, P., and Gordon, S. (1990). Evidence that Very Slow Wallerian Degeneration in C57BL/Ola Mice is an Intrinsic Property of the Peripheral Nerve. *Eur. J. Neurosci.* 2, 802–808.
- Glass, J.D., Brushart, T.M., George, E.B., and Griffin, J.W. (1993). Prolonged survival of transected nerve fibres in C57BL/Ola mice is an intrinsic characteristic of the axon. *J. Neurocytol.* 22, 311–321.
- Gillingwater, T.H., Ingham, C.A., Parry, K.E., Wright, A.K., Haley, J.E., Wishart, T.M., Arbuthnott, G.W., and Ribchester, R.R. (2006). Delayed synaptic degeneration in the CNS of WldS mice after cortical lesion. *Brain* 129, 1546–1556.
- Mack, T.G., Reiner, M., Beirowski, B., Mi, W., Emanuelli, M., Wagner, D., Thomson, D., Gillingwater, T., Court, F., Conforti, L., et al. (2001). Wallerian degeneration of injured axons and synapses is delayed by a Ube4b/Nmnat chimeric gene. *Nat. Neurosci.* 4, 1199–1206.
- Avery, M.A., Sheehan, A.E., Kerr, K.S., Wang, J., and Freeman, M.R. (2009). Wld S requires Nmnat1 enzymatic activity and N16-VCP interactions to suppress Wallerian degeneration. *J. Cell Biol.* 184, 501–513.
- Yahata, N., Yuasa, S., and Araki, T. (2009). Nicotinamide mononucleotide adenyltransferase expression in mitochondrial matrix delays Wallerian degeneration. *J. Neurosci.* 29, 6276–6284.
- George, E.B., Glass, J.D., and Griffin, J.W. (1995). Axotomy-induced axonal degeneration is mediated by calcium influx through ion-specific channels. *J. Neurosci.* 15, 6445–6452.
- Yi, M., Weaver, D., and Hajnóczky, G. (2004). Control of mitochondrial motility and distribution by the calcium signal: a homeostatic circuit. *J. Cell Biol.* 167, 661–672.
- Wang, X., and Schwarz, T.L. (2009). The mechanism of Ca<sup>2+</sup>-dependent regulation of kinesin-mediated mitochondrial motility. *Cell* 136, 163–174.
- Russo, G.J., Louie, K., Wellington, A., Macleod, G.T., Hu, F., Panchumarthi, S., and Zinsmaier, K.E. (2009). Drosophila Miro is required for both anterograde and retrograde axonal mitochondrial transport. *J. Neurosci.* 29, 5443–5455.
- Ganitkevich, V.Y. (2003). The role of mitochondria in cytoplasmic Ca<sup>2+</sup> cycling. *Exp. Physiol.* 88, 91–97.
- Brown, M.R., Sullivan, P.G., Dorenbos, K.A., Modafferi, E.A., Geddes, J.W., and Steward, O. (2004). Nitrogen disruption of synaptosomes: an alternative method to isolate brain mitochondria. *J. Neurosci. Methods* 137, 299–303.
- Naga, K.K., Sullivan, P.G., and Geddes, J.W. (2007). High cyclophilin D content of synaptic mitochondria results in increased vulnerability to permeability transition. *J. Neurosci.* 27, 7469–7475.
- Sasaki, Y., and Milbrandt, J. (2010). Axonal degeneration is blocked by nicotinamide mononucleotide adenyltransferase (Nmnat) protein transduction into transected axons. *J. Biol. Chem.* 285, 41211–41215.
- Knöferle, J., Koch, J.C., Ostendorf, T., Michel, U., Planchamp, V., Vutova, P., Tönges, L., Stadelmann, C., Brück, W., Bähr, M., and Lingor, P. (2010). Mechanisms of acute axonal degeneration in the optic nerve in vivo. *Proc. Natl. Acad. Sci. USA* 107, 6064–6069.
- Santo-Domingo, J., and Demarex, N. (2010). Calcium uptake mechanisms of mitochondria. *Biochim. Biophys. Acta* 1797, 907–912.
- Sievers, C., Platt, N., Perry, V.H., Coleman, M.P., and Conforti, L. (2003). Neurites undergoing Wallerian degeneration show an apoptotic-like process with Annexin V positive staining and loss of mitochondrial membrane potential. *Neurosci. Res.* 46, 161–169.
- Sunio, A., and Bittner, G.D. (1997). Cyclosporin A retards the wallerian degeneration of peripheral mammalian axons. *Exp. Neurol.* 146, 46–56.
- Barrientos, S.A., Martinez, N.W., Yoo, S., Jara, J.S., Zamorano, S., Hetz, C., Twiss, J.L., Alvarez, J., and Court, F.A. (2011). Axonal degeneration is mediated by the mitochondrial permeability transition pore. *J. Neurosci.* 31, 966–978.
- Pandya, J.D., Pauly, J.R., and Sullivan, P.G. (2009). The optimal dosage and window of opportunity to maintain mitochondrial homeostasis following traumatic brain injury using the uncoupler FCCP. *Exp. Neurol.* 218, 381–389.
- Pandya, J.D., Pauly, J.R., Nukala, V.N., Sebastian, A.H., Day, K.M., Korde, A.S., Maragos, W.F., Hall, E.D., and Sullivan, P.G. (2007). Post-Injury Administration of Mitochondrial Uncouplers Increases Tissue Sparing and Improves Behavioral Outcome following Traumatic Brain Injury in Rodents. *J. Neurotrauma* 24, 798–811.
- Ikegami, K., and Koike, T. (2003). Non-apoptotic neurite degeneration in apoptotic neuronal death: pivotal role of mitochondrial function in neurites. *Neuroscience* 122, 617–626.
- Schon, E.A., and Przedborski, S. (2011). Mitochondria: the next (neuro)degeneration. *Neuron* 70, 1033–1053.
- De Vos, K.J., Chapman, A.L., Tennant, M.E., Manser, C., Tudor, E.L., Lau, K.F., Brownlee, J., Ackerley, S., Shaw, P.J., McLoughlin, D.M., et al. (2007). Familial amyotrophic lateral sclerosis-linked SOD1 mutants perturb fast axonal transport to reduce axonal mitochondria content. *Hum. Mol. Genet.* 16, 2720–2728.
- Shi, P., Ström, A.L., Gal, J., and Zhu, H. (2010). Effects of ALS-related SOD1 mutants on dynein- and KIF5-mediated retrograde and anterograde axonal transport. *Biochim. Biophys. Acta* 1802, 707–716.
- Wang, X., Su, B., Zheng, L., Perry, G., Smith, M.A., and Zhu, X. (2009). The role of abnormal mitochondrial dynamics in the pathogenesis of Alzheimer's disease. *J. Neurochem.* 109 (Suppl 1), 153–159.
- Chang, D.T., Rintoul, G.L., Pandipati, S., and Reynolds, I.J. (2006). Mutant huntingtin aggregates impair mitochondrial movement and trafficking in cortical neurons. *Neurobiol. Dis.* 22, 388–400.